Broad-band magnetic brain activity during rhythmic tapping tasks

T. Holroyd[1], M. Nielsen[1], S. Miyauchi[1], and T. Yanagida[1,2]

[1]*Kansai Advanced Research Ctr., Communications Research Lab., 588-2 Iwaoka, Nishi-ku, Kobe 651-2492, Japan;* [2]*Dept. of Physiology I, Osaka Univ. Medical School, 2-2 Yamadaoka, Suita, Osaka 565-0871, Japan*

1 Introduction

Humans are able to generate and maintain rhythmic activity (as in running or beating a drum) and can also synchronize an internally generated rhythm with an external one. Brain functions involved in this ability include at least: internal rhythm generation, prediction of anticipated rhythmic stimuli, movement planning and timing, and coordination of the brain areas responsible for these functions. Several magnetoencephalographic (MEG) studies have implicated various brain areas in the ability to perform rhythmic tasks, including right frontal cortex [1], primary and secondary auditory cortices [2], and right frontal, premotor, and secondary auditory areas [3]. Functional magnetic resonance imaging (fMRI), positron emission tomography (PET), and lesion studies [4, 5, 6] have also demonstrated the involvement of these areas during timing and synchronization tasks.

In this paper, we investigate the magnetic brain activity of subjects performing two rhythmic tapping and synchronization tasks. We use an adaptive linear-filtering technique known as *differential synthetic-aperture magnetometry* (dSAM) to locate sources of activity that have high signal-to-noise power ratios in various frequency bands. We then project the whole brain activity onto the individual sources with SAM spatial filters and examine the projections for evidence of phase-synchrony between the different sources. By isolating the oscillatory electromagnetic signals produced by the brain during performance, we can investigate the hypothesis that coordination between brain areas may be accomplished via phase-locking of the oscillatory activity.

2 Methods

2.1 Experiments

Exp. 1: Missing Stimulus. Two subjects, one male and one female, were instructed to synchronize right (preferred) index-finger flexions with an auditory metronome that had a fixed period of 800 msec (1.25 Hz). The metronome pulses were 80 msec 1 kHz tones. The 800 msec period has been shown to be very stable in such synchronization tasks; even if a stimulus is omitted, subjects will continue tapping synchronously with the metronome [7]. In order to do this, subjects must predict the time of an upcoming metronome beat and plan a movement to occur at the same time. Brain structures that are responsible for the internal representation of the metronome rhythm and for motor planning must therefore be active during the task. We randomly omitted 12% of the stimuli in order to probe these brain structures. Subjects performed 21 blocks of 40 cycles each, yielding approximately 100 missing-stimulus responses.

Exp. 2: Constant vs. Random. In this experiment, the metronome produced alternating 15-cycle trials of either constant 800 msec cycles or random 400–1200 msec cycles with a mean of 800 msec. Three subjects (who did not participate in Exp. 1), two male and one female, were instructed to synchronize right index-finger flexions with the metronome during the constant period trials and to continue at the same tapping frequency during the random period trials. There were 16 trials (8 of each condition); the first three cycles of each trial were discarded to avoid transient effects. When the metronome period was random, subjects were required to use their internal memory of the rhythm to produce constant period tapping. By comparing the differences in brain activity between the two conditions, we can locate brain structures which are active during internal rhythm generation and self-paced movements, as well as areas related to external attention and synchronization. Auditory-only trials were also recorded in both experiments.

Magnetic brain activity was recorded using a whole-head MEG system consisting of 148 radial magnetometers (BTi Magnes). The data were sampled at a rate of 678 Hz using a high-pass filter with a low-frequency cutoff of 0.1 Hz. The MEG system was located in a magnetically shielded room (Siemens) placed on an active vibration-damping floor. MEG data were digitally filtered off-line in several frequency bands including 15–25 Hz, 18–22 Hz, and 38–42 Hz. Narrow bands are required for the phase analysis.

2.2 Differential SAM

SAM filters are optimized to produce the highest possible signal-to-noise ratio for a given oscillatory source in the brain [8].

$$\begin{aligned} \mathbf{h} &= \frac{\mathbf{C}^{-1}\mathbf{g}}{\mathbf{g}^T\mathbf{C}^{-1}\mathbf{g}} \\ \xi &= \mathbf{h}^T\mathbf{X} \\ S^2 &= \mathbf{h}^T\mathbf{C}\mathbf{h} \end{aligned}$$

where $\mathbf{C}$ is the covariance matrix $\mathbf{X}\mathbf{X}^T$ of the bandpass filtered raw MEG data $\mathbf{X}$ (sensors $\times$ time), $\mathbf{g}$ is a column vector containing the theoretical magnetic field generated by a given fixed source, $\mathbf{h}$ is the SAM filter, ξ is the resulting estimate of source activity, and S^2 is the source power estimate. The covariance matrix was regularized by adding 5 times its smallest eigenvalue to each element of the diagonal.

Differential SAM (dSAM) compares the level of source activity between *active* (a) and *control* (c) conditions, by computing the covariances and source power estimates separately and using the statistic $\rho = \sqrt{S_a^2/S_c^2}$. For large N, ρ is distributed approximately normally about a mean of 1. Sources with ρ values in the tails of this distribution are said to be *differentially activated* by the different conditions. We used a cutoff of $p < .01$ to determine active sources.

2.3 Timeseries Analysis: Phase Locking

The *Hilbert transform* $x \Rightarrow z$ is defined as follows:

$$\begin{aligned} x &\Rightarrow \widehat{x} \\ \widehat{z} &= \begin{cases} \widehat{x} \times 2 & \text{if } f > 0 \\ 0 & \text{if } f < 0 \end{cases} \\ \widehat{z} &\Rightarrow z \end{aligned}$$

where $\Rightarrow$ represents the Fourier transform.

If the Hilbert transform is applied to a bandpass-filtered real timeseries x, the result is a complex timeseries z such that the real part is the original timeseries x and the imaginary part is x phase-shifted by 90°. The envelope of the original timeseries may therefore be calculated as $|z|$.

Given the Hilbert transform z of a timeseries x, the *complex phase*

$$\phi = \frac{z}{|z|}$$

is an estimate of the instantaneous phase of x at any given time. Given the complex phases from two different timeseries x and y, their *relative phase* θ may be written as

$$\theta = \frac{\phi_2}{\phi_1}.$$

The complex relative phase θ may be averaged over cycles to give the *phase-locking value* (PLV), a measure of the extent to which the two timeseries are phase-locked [9].

$$\text{PLV} = \frac{1}{N}\left|\sum_{i=1}^{N}\theta(i)\right|$$

The PLV for a given point in time is the length of the average relative phase vector in the complex plane (all the $\theta(i)$ have length 1). When two timeseries are phase-locked, the $\theta(i)$ will be approximately equal, and the PLV will approach 1. When the $\theta(i)$ are scattered randomly around the unit circle, the PLV will approach 0.

In order to determine whether the PLV is statistically significant or not, we use a bootstrapping technique in which surrogate data are generated by shuffling the cycles of one of the timeseries [9]. If the two timeseries are phase-locked *within* each cycle, but have varying absolute phases *across* cycles, then shuffling the cycles will destroy the phase-locking relationship and the PLV will be small. The *phase-locking statistic* (PLS) is defined as the standard deviation of the shuffled PLV values. The H_0-hypothesis that the two timeseries are not phase-locked may be rejected if the original (unshuffled) PLV is larger than some multiple of the PLS, typically 3.

2.4 MRI-based Cortical Source Modeling

SAM depends on an accurate current source model in order to calculate theoretical magnetic fields. We used the FreeSurfer package [10] to prepare white-matter surface models from structural MRI scans of the subject's brains. 50,000 dipole sources were scattered randomly over the white-matter surfaces and oriented perpendicularly to them. Magnetic fields were calculated using the homogeneous spherical conductor formula [11].

3 Results

3.1 Behavior

In Exp. 1, both subjects were able to produce 1–1 tapping. Mean Δt ± SD (msec): S$_1$, -186 ± 91; S$_2$, -194 ± 54. In Exp. 2, one subject (S$_1$) did not synchronize with the metronome at any time. The other two were able to synchronize during the constant

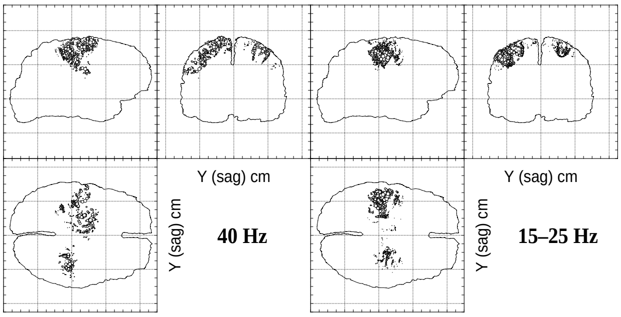

Figure 1: *Active sources (S_1, Exp. 1) for the auditory-only vs. tapping contrasts in two frequency bands. All sources are significant at the $p < .01$ level, and include left and right central and precentral sulci.*

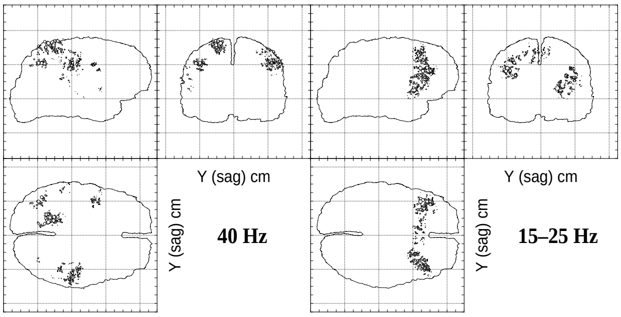

Figure 2: *Left: sources that were active during tapping, including left central and intraparietal sulci. Right: sources that were active for the missing stimulus, including left and right inferior frontal cortex.*

condition and reproduce the rhythm during the random condition. Mean IRI ± SD (msec): S_2, 804 ± 45; S_3, 806 ± 67 (constant); S_2, 765 ± 73; S_3, 814 ± 82 (random).

3.2 Differential SAM

Fig. 1 shows primarily sensorimotor sources that were more active in the auditory-only condition than in the tapping condition, probably due to desynchronization during tapping. In Fig. 2 the missing stimulus activated BA44/45, while parietal and motor areas were desynchronized. Fig. 3 shows activation of right frontal cortex by the constant metronome and the left frontal cortex during internal rhythm generation (tapping) in the random condition.

3.3 Phase Synchrony

Both subjects in Exp. 1 had active sources in right superior frontal and left central cortices. The PLV values between these sources are shown in Fig. 4. Because there were fewer cycles in the missing stimulus condition, the PLS values are much higher than for the normal condition, so it is unclear whether there was enhanced desynchronization prior to the movement or enhanced synchronization at -250 msec. Fig. 5 shows a constant vs. random contrast. Note the enhanced phase-locking in the random condition prior to movement. Also, the metronome had a desynchronizing effect (visible only in the constant condition since tapping was synchronized).

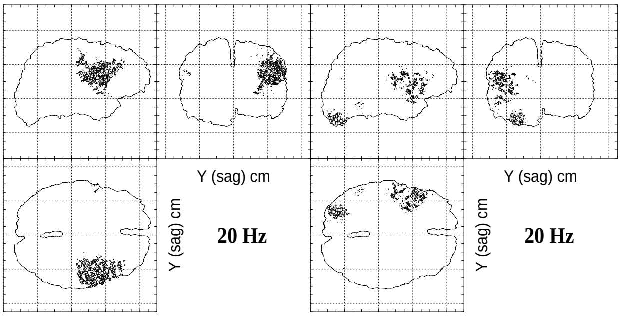

Figure 3: *Active sources for S_2 in Exp. 2. Left: constant vs. random in the auditory-only condition: right precentral and inferior frontal areas. Right: tapping vs. auditory-only during random trials: left inferior frontal and precentral areas.*

4 Discussion

We used rhythmic tapping tasks to establish patterns of coordination within the brain. By perturbing these patterns, we created contrasts that could be analyzed with differential SAM. We located sources in the right and left inferior frontal cortices that were activated by missing stimuli and internal rhythm generation, and which were phase-coupled with left precentral and central areas.

Central and precentral areas were active bilaterally during unimanual tapping and exhibited temporally relevant variations in frequency and phase-synchrony with other regions, suggesting that ipsilateral central cortex may help mediate sensorimotor coordination.

Additional active regions included occipital cortex (but not V1) and bilateral parietal regions (BA40/7, BA39), which also showed phase-locking with motor areas and may contribute to internal timing.

Subject variability in patterns of inter-area phase-coupling may reflect differences in network organization related to task strategies or performance skill. Frontal regions especially were variable from subject to subject which may indicate differences in internal

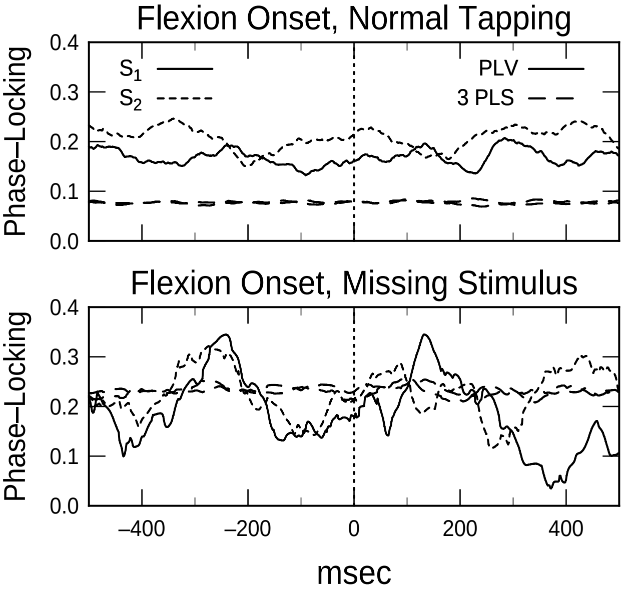

Figure 4: *PLV values between right superior frontal and left central cortices in Exp. 1 (both subjects). Values above 3 PLS are significant. Vertical dotted lines show flexion onset. 40 Hz band.*

rhythm generation strategies.

Both event-related synchronization and desynchronization were observed, depending on modality and frequency. Some areas displayed almost continuous significant phase locking with event-related modulation. Correlated oscillatory activity may therefore signal the binding of populations of neurons while changes in the observed phase-couplings would indicate the flow of information between brain areas.

References

[1] S.-L. Joutsiniemi and R. Hari. Omissions of auditory stimuli may activate frontal cortex. *Eur. J. Neurosci.*, **1**:524–528, 1989.

[2] S. Miyauchi, R. Takino, Y. Sasaki, B. Pütz, and H. Okamura. Missing auditory stimuli activate the primary and periauditory cortices: combining MEG and fMRI studies. *Electroenceph. clin. Neurophysiol. Suppl.*, **47**:233–239, 1996.

[3] T. Holroyd, T. Takeda, T. Masuda, and N. Harada. Broad-band activity within a distributed brain network during a sensorimotor synchronization task. *Soc. Neurosci. Abst.*, **25**, 1999.

[4] S. M. Rao, D. L. Harrington, K. Y. Haaland, J. A. Bobholz, R. W. Cox, and J. R. Binder. Distributed neural systems underlying the timing of movements. *J. Neurosci.*, **17**:5528–5535, 1997.

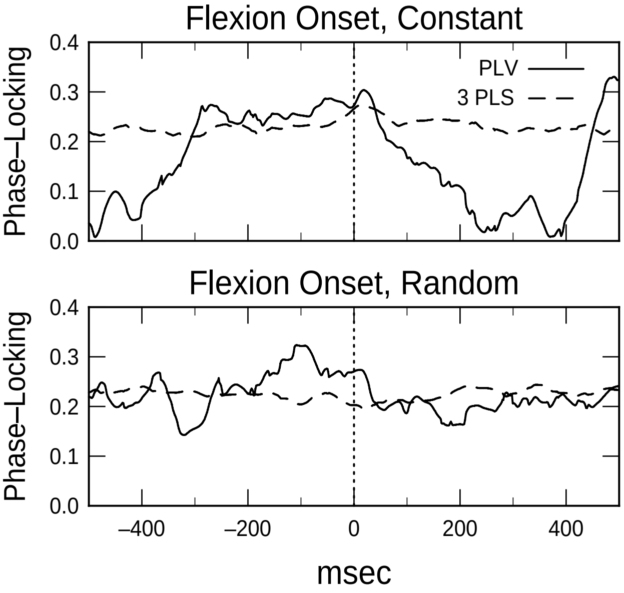

Figure 5: *PLV values for Exp. 2 (S_1) between left inferior frontal and central cortices. 20 Hz band.*

[5] R. J. Zatorre, A. R. Halpern, D. W. Perry, E. Meyer, and A. C. Evans. Hearing in the mind's ear: a PET investigation of musical imagery and perception. *J. Cognit. Neurosci.*, **8**:29–46, 1996.

[6] D. L. Harrington, K. Y. Haaland, and R. T. Knight. Cortical networks underlying mechanisms of time perception. *J. Neurosci.*, **18**:1085–1095, 1998.

[7] D. A. Engström, J. A. S. Kelso, and T. Holroyd. Reaction-anticipation transitions in human perception-action patterns. *Hum. Mov. Sci.*, **15**:809–832, 1996.

[8] S. E. Robinson and J. Vrba. Functional neuroimaging by synthetic aperture magnetometry (SAM). In *Recent Advances in Biomagnetism*, T. Yoshimoto, M. Kotani, S. Kuriki, N. Nakasato, and H. Karibe, eds., Sendai: Tohoku University Press, 1999, pp. 302–305.

[9] J.-P. Lachaux, E. Rodriguez, J. Martinerie, and F. J. Varela. Measuring phase synchrony in brain signals. *Hum. Brain Map.*, **8**:194–208, 1999.

[10] A. M. Dale, Bruce Fischl, and M. I. Sereno. Cortical surface-based analysis I: Segmentation and surface reconstruction. *NeuroImage*, **9**:179–194, 1999.

[11] J. Sarvas. Basic mathematical and electromagnetic concepts of the biomagnetic inverse problem. *Phys. Med. Biol.*, **32**:11–22, 1987.